P2.1 **Atmospheric Waves Associated with a Valley of Lantau Island: Observation, Theory and Numerical Simulation**

P.W. Chan *
Hong Kong Observatory, Hong Kong, China

1. INTRODUCTION

The Hong Kong Observatory (HKO) operates a Doppler LIght Detection And Ranging (LIDAR) system at the Hong Kong International Airport (HKIA) for providing windshear alerts to aircraft. Besides measuring the winds along the runways, the LIDAR is also used to study disturbances in the airflow downstream of the complex terrain of Lantau Island, a mountainous island to the south of HKIA (Figure 1). For this purpose, vertical cross-sectional scans are made regularly across Tung Chung Gap, a valley of about 370 m AMSL near the middle of Lantau Island (location in Figure 1).

The cross sectional scans are found to give many interesting observations of waves in the cross-valley airflow. This paper describes two examples, namely, stationary lee wave downstream of the valley in the prevailing east to southeasterly airstream, and upstream propagating wave during the prevalence of northwesterly wind. The LIDAR observations are compared with theoretical description of the waves and, when available, numerical simulation results.

Figure 1 Map of HKIA and Lantau Island (height contours: 100 m). The LIDAR is marked by a red square, with the direction of the Tung Chung Gap vertical scanning indicated by a pink arrow.

2. STATIONARY LEE WAVE

In the morning of 23 February 2004, a ridge of high pressure with closely packed surface isobars dominated over the southeastern coast of China (Figure 2). Strong easterly wind prevailed over Hong Kong. The wind veered slowly with altitude so that the hilltops on Lantau Island (up to 1 km AMSL) recorded basically easterly wind as well. There was a southeasterly jet between 1 and 2 km above ground.

From the LIDAR cross-sectional scan at Tung Chung Gap in that morning (Figure 3), there were two "slanting" areas of reversed/tangential flow embedded in the prevailing easterly below the southeasterly jet. The LIDAR's backscattered power plot (Figure 4) suggests that there is a wave between 500 and 1000 m AMSL or so extending for two wavelengths downstream of Tung Chung Gap. The wave seems to be associated with the "slanting" reversed/tangential flow in the radial velocity plot. It is basically stationary in time with a wavelength of about 2.8 km.

The wave observed in the cross-sectional scan of the LIDAR is compared with linear wave theory. Vertical profiles of the cross wind (i.e. component of the wind along 160°, perpendicular to the mountain ranges on Lantau Island) and the temperature upstream of Lantau Island are provided by a wind profiler and a microwave radiometer respectively, and they are shown in Figure 5. The Scorer parameter profile is computed from these data. It could be approximated by a three-layer structure, as in the fitted Scorer parameter profile in Figure 5. Based on Zang and Zhang (2004) which extended the 2-layer formulation of Scorer (1949) to 3 layers, assuming that the troposphere is composed of 3 layers with constant Scorer parameters l_1 (bottom), l_2 (middle) and l_3 (upper) satisfying the following relationship:

$$l_1^2 \le l_3^2 < l_2^2 \qquad (1)$$

and that the middle and bottom layers have the same depth h, the wavenumber k can be calculated from:

$$\cot(\gamma_2 h) + \frac{(\mu_1\mu_3/\gamma_2) - \gamma_2 th(\mu_1 h)}{\mu_1 + \mu_3 th(\mu_1 h)} = 0 \qquad (2)$$

where $\mu_i = \sqrt{k^2 - l_i^2}$ for i = 1 and 3, $\gamma_2 = \sqrt{l_2^2 - k^2}$ and $th(x)$ is hyperbolic tangent. Taking l_1^2=4.78x10^{-6} m^{-2}, l_2^2=5.6x10^{-5} m^{-2}, l_3^2= 5.1x10^{-6} m^{-2} and h = 500 m from Figure 5, the wavelength is found to be 2.7 km, which is close to the LIDAR observation. Moreover, it could be readily verified that the Scorer parameter values satisfy the following conditions of the occurrence of lee wave in a three-layer atmosphere (Zang and Zhang 2005):

$$0 < l_2^2 - l_3^2 < \frac{\pi^2}{4h^2} < \frac{\pi^2}{4h^2}[1 + th(h\sqrt{l_2^2 - l_1^2})] \qquad (3)$$

$$l_3^2 - l_1^2 < l_2^2 - l_1^2 < \frac{\pi^2}{4h^2} < \frac{\pi^2}{4h^2}[1 + th(h\sqrt{l_2^2 - l_1^2})] + l_3^2 - l_1^2 \qquad (4)$$

To further understand the lee wave, numerical simulation is also performed using the upstream wind and temperature profiles in the homogeneous

* *Corresponding author address:* P.W. Chan, Hong Kong Observatory, 134A Nathan Road, Hong Kong email: pwchan@hko.gov.hk

initialization run of the Regional Atmospheric Modelling System version 4.4 (Szeto and Chan 2006). The wind distribution across Tung Chung Gap in the simulation is shown in Figure 6. It could be seen that the wave features revealed by the LIDAR observations are reproduced very well by the simulation. The first area of reversed/tangential flow just downstream of the valley is related to upslope, rotor-like flow. The second area is depicted as the upward motion in a wave crest.

3. UPSTREAM PROPAGATING WAVE

Under the combined effect of the northeast monsoon and Tropical Storm Damrey, moderate northwesterly wind prevailed along the south China coast in the morning of 22 September 2005 (Figure 7). Higher up in the boundary layer, winds up to strong force were observed on the LIDAR scan towards Tung Chung Gap between 500 and 1000 m AMSL (right panels in Figure 8). Visibility gradually deteriorated at HKIA in haze and the backscatter power plot of the LIDAR across Tung Chung Gap shows a distinct layer of denser aerosol (left panels in Figure 8). In a period of about 79 minutes, a wave appeared to propagate upstream against the background northwesterly flow as shown in both the backscatter power and radial velocity plots that were updated in 1.5 – 4 minutes (Figure 8). At the same time, part of the jump-like feature of the airflow downstream of the Tung Chung Gap could be observed (right panels, Figure 8). The speed of wave propagation is about 1.1 m/s and peak-to-peak distance in the wave train is about 5.4 km.

The upstream propagating wave and the jump-like feature look very similar to the soliton model in a two-layer system in the study of airflow impinging on an island (Li et al. 2004). The soliton is described by a non-dimensional two layer forced Korteweg-de Vries (fKdV) equation as given by:

$$\frac{\partial \eta}{\partial t} + (F-1)\frac{\partial \eta}{\partial x} - \frac{3}{2}\delta d_{-2}\eta\frac{\partial \eta}{\partial x} - \frac{1}{6}\beta d_1\frac{\partial^3 \eta}{\partial x^3} = \frac{\gamma F}{2\delta d_{-1}}\frac{dh}{dx} \quad (5)$$

where η is the nondimensional interface displacement, h is the nondimensional height of the topography, $F = U/c_0$ is the Froude number, $c_0 = \sqrt{g' h_0}$ is the phase speed of linear nondispersion long wave, g' is the reduced gravity acceleration, $h_0 = \frac{d_m d_p}{d_m + d_p}$ is the characteristic depth of the atmosphere, d_m and d_p are the thickness of the lower and upper layers respectively, $\delta = a/h_0$ where a is the characteristic displacement of the interface and δ is the measure of nonlinearity, $\beta = (h_0/l)^2$ where l is the characteristic length of the topography, $\gamma = H_0/h_0$ where H_0 is the characteristic height of the topography, $d_n = d_-^n + (-1)^{n-1} d_+^n$ where $d_+ = d_p/h_0$ and $d_- = d_m/h_0$.

The parameters in Eq. (5) take the following values based on the 00 UTC (HKT = UTC + 8 hours) radiosonde ascent data in Hong Kong on 22 September 2005 (Figure 9): U = 11.3 m/s, g' = 0.15, d_m = 1000 m, d_p = 4000 m, h_0 = 800 m, c_0 = 11 m/s, F = 1.03, a = 125 m, δ = 0.16, l = 2 km, β = 0.16, H_0 = 370 m, and γ = 0.46. In particular, the values of d_m and d_p are so selected to give the h_0 of 800 m, which is the altitude of the isothermal layer at the top of the boundary layer (see the inset of Figure 9) that appears to be associated with the subsidence due to Tropical Storm Damrey. This is also about the height of the denser aerosol in the cross-sectional scan at Tung Chung Gap from the LIDAR (left panels of Figure 8).

Using the above parameters, the solution to Eq. (5) is shown in Figure 10. The appearance and movement of the wave at negative x-axis are reminiscent of the wave train revealed in Figure 8. The phase speed of the soliton is estimated to be 0.95 m/s. The peak-to-peak distance in the wave train is about 6.25 km. Both values are close to the actual observations.

A sensitivity study has also been conducted on the effect of the input parameters to the solution of Eq. (5). For instance, if a value of 700 m is adopted for h_0, we may use d_m = 1000 m and d_p = 2333 m. The solution is similar to Figure 10. If a value of 600 m is adopted for h_0, we may use d_m = 700 m and d_p = 4300 m. In that case, the phase speed of the soliton is found to be doubled (about 1.9 m/s), but is still of the same order of magnitude of the observed value. The peak-to-peak distance in the wave train remains about the same (not shown). It looks like d_m = 1000 m is a more reasonable choice to represent the typical height of the boundary layer.

4. CONCLUSIONS

Two examples of wave motion across Tung Chung Gap are documented in this paper using the vertical scanning data from the LIDAR, namely, a lee wave downstream of the valley in prevailing east to southeasterly flow, and upstream propagating wave during the prevalence of northwesterly airstream. Both backscatter power data and radial velocity measurement of the LIDAR depict the occurrence and evolution of these waves. For the lee wave, the observation is consistent with the prediction of linear wave theory in a three-layer model. Numerical simulation by homogeneous initialization also sheds light on the structure of the wave. For the upstream propagating wave, soliton model in a two-layer system as described by a forced KdV equation appears to offer a reasonable description of the phenomenon. The phase speed of the soliton and the peak-to-peak distance in the wave train as predicted by this model are generally consistent with the actual observations. The results in this paper could be used as conceptual models to understand the airflow across Tung Chung Gap in the day-to-day monitoring of the wind at the airport area.

Acknowledgement

The author would like to thank Dr. Xiaofeng Li of NESDIS/NOAA for useful discussions of upstream propagating waves.

References

Li, X., C. Dong, P. Clemente-Colon, W. G. Pichel, and K. S. Friedman, 2004: Synthetic aperture radar observation of the sea surface imprints of upstream atmospheric solitons generated by

flow impeded by an island. *J. Geophys. Res.*, **109**, C02016-C02023.

Scorer, R.S., 1949: Theory of waves in the lee of mountains. *Quart. J. Roy. Meteor. Soc.*, **75**, 41-56.

Szeto, K.C., and P.W. Chan, 2006: High resolution numerical modelling of windshear episodes at the Hong Kong International Airport. *12th Conference on Aviation, Range, and Aerospace Meteorology*, American Meteorological Society, Georgia, U.S.A.

Zang, Z., and M. Zhang, 2004: Theoretical study on trapped lee waves on three layers model. *Acta Meteorologica Sinica*, **62**, 395-400 (in Chinese with English abstract).

Zang, Z., and M. Zhang, 2005: Theoretical analysis of the existent condition of lee waves in three-layer model. *Journal of Hydrodynamics*, **20**, 577-584 (in Chinese with English abstract).

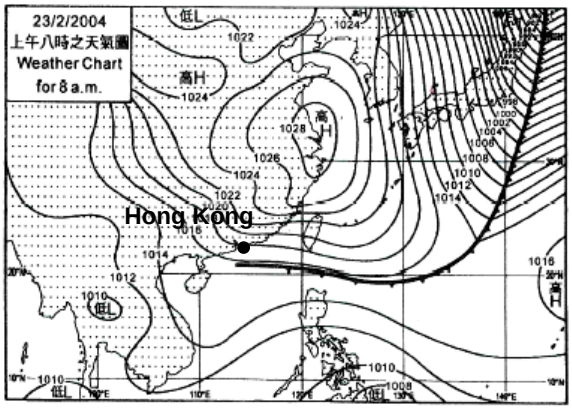

Figure 2 Surface isobaric chart at 8 a.m., 23 February 2004.

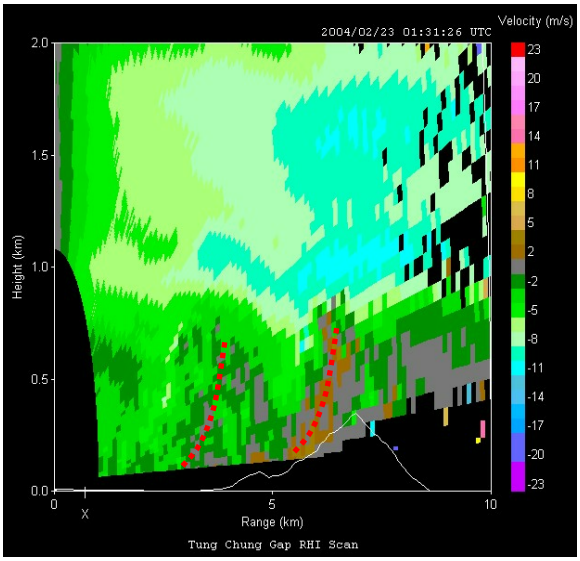

Figure 3 Radial velocity image of the LIDAR's cross section at Tung Chung Gap at 9:31 a.m., 23 February 2004.

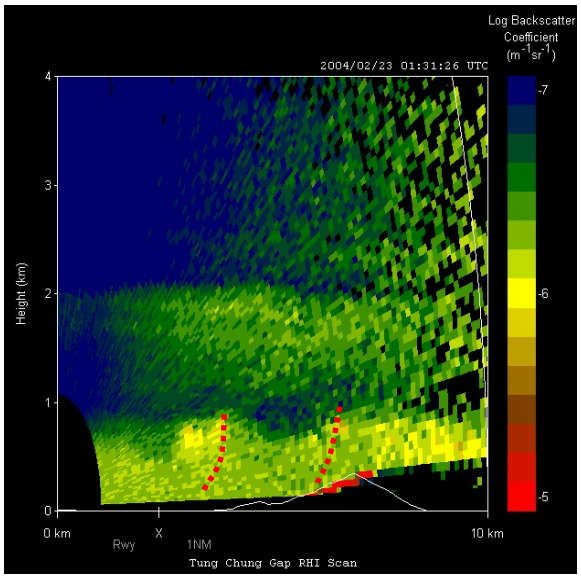

Figure 4 Backscatter power plot of the LIDAR's cross section at Tung Chung Gap at 9:31 a.m., 23 February 2004.

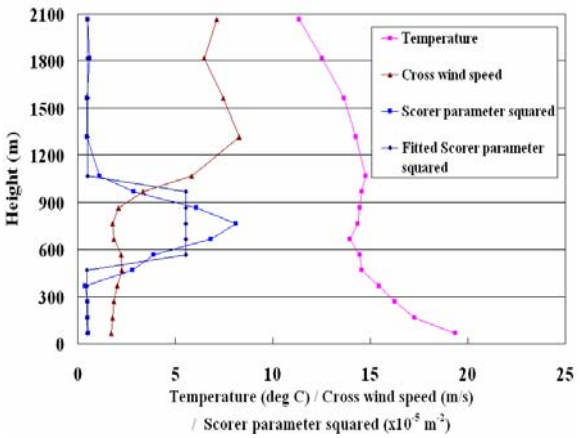

Figure 5 Vertical profiles of temperature, cross wind speed and Scorer parameter squared based on wind profiler and radiometer data at 10 a.m., 23 February 2004.

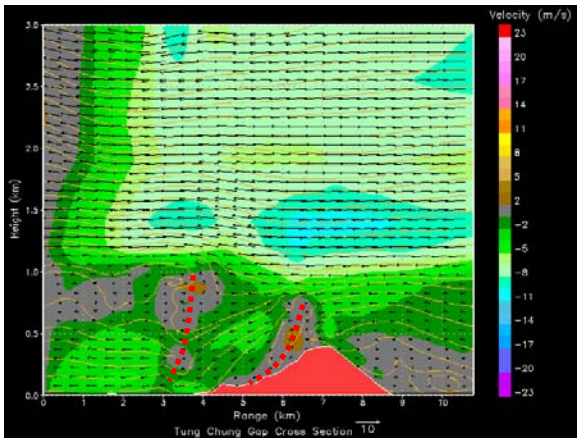

Figure 6 Numerical simulation result of the wind component projected on the Tung Chung Gap cross section (arrow) and the velocity resolved along the LIDAR's measurement radial (shaded contours).

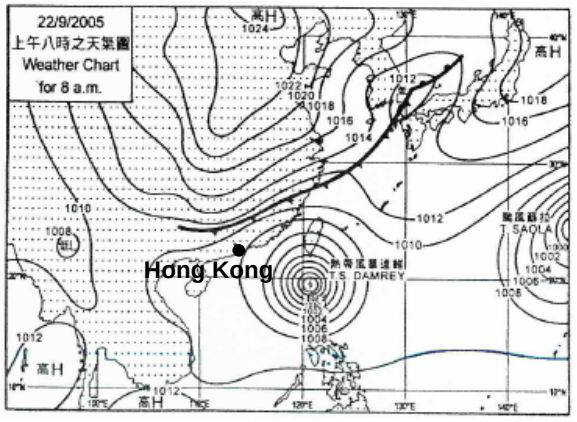

Figure 7 Surface isobaric chart at 8 a.m., 22 September 2005.

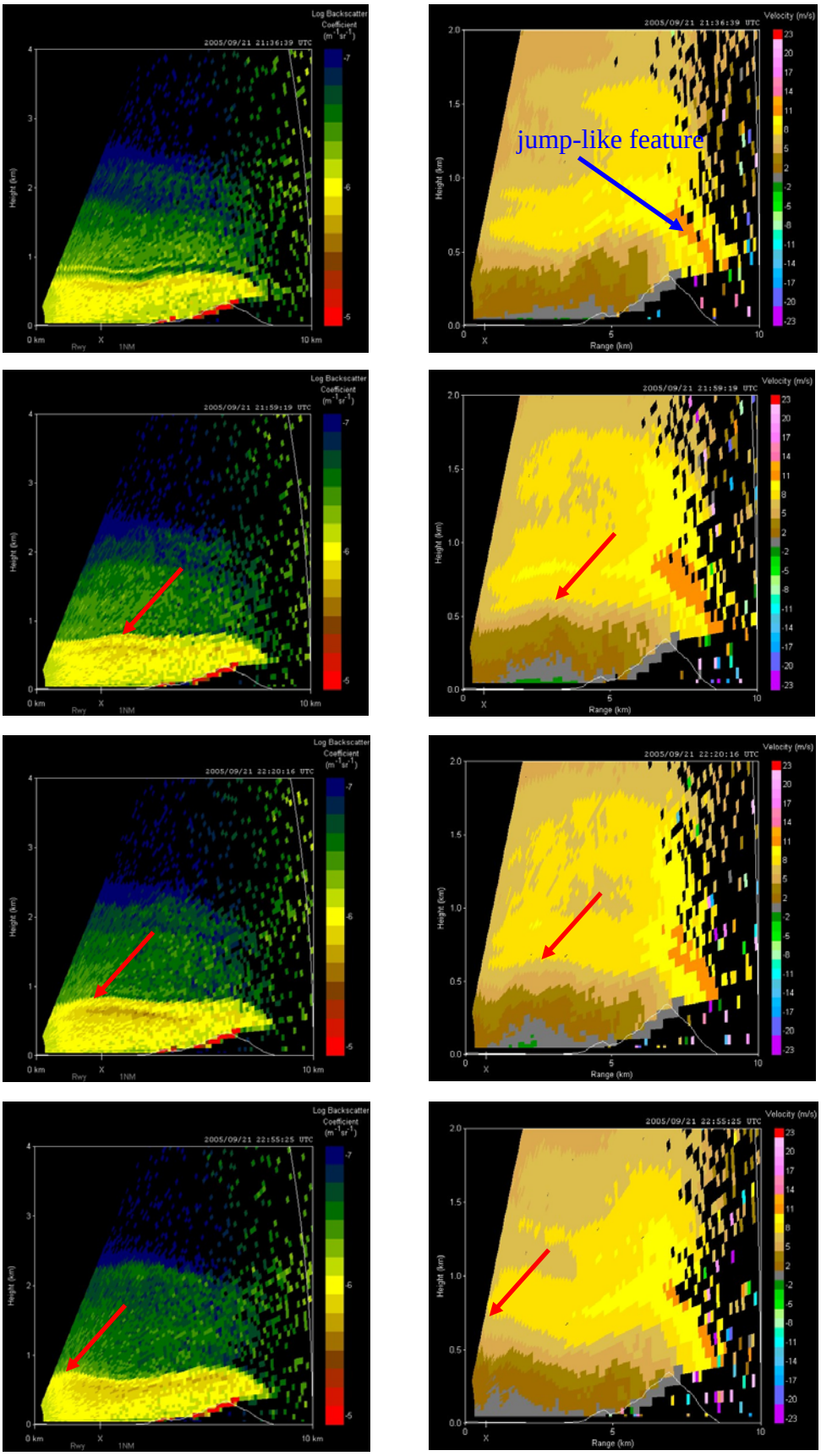

Figure 8 Backscatter power plots (left panels) and radial velocity plots (right panels) across Tung Chung Gap between 5:36 and 6:55 a.m., 22 September 2005. The upstream propagating wave is indicated by a red arrow.

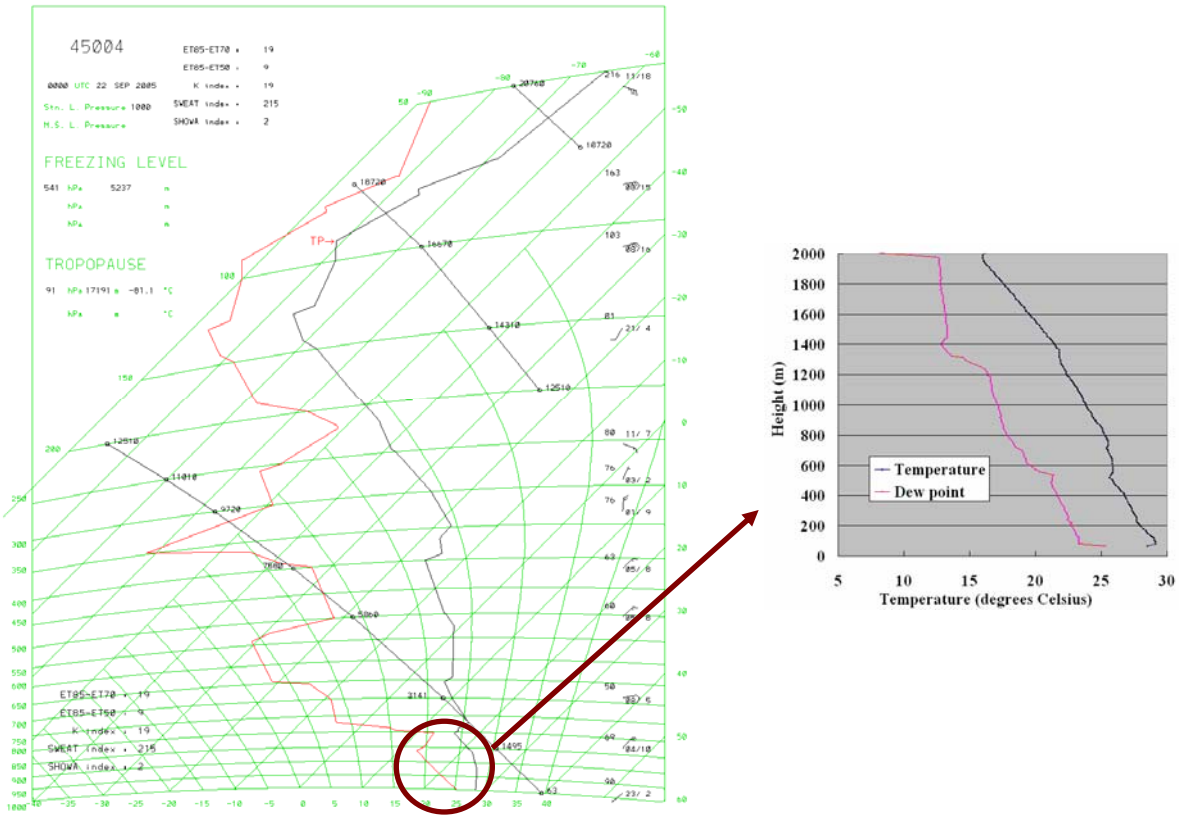

Figure 9 Tephigram of Hong Kong at 00 UTC (8 a.m. HKT), 22 September 2005. The black curve is the temperature profile and the red curve is the dew point profile. A zoom-in of the part of the tephigram within the boundary layer is given in the inset.

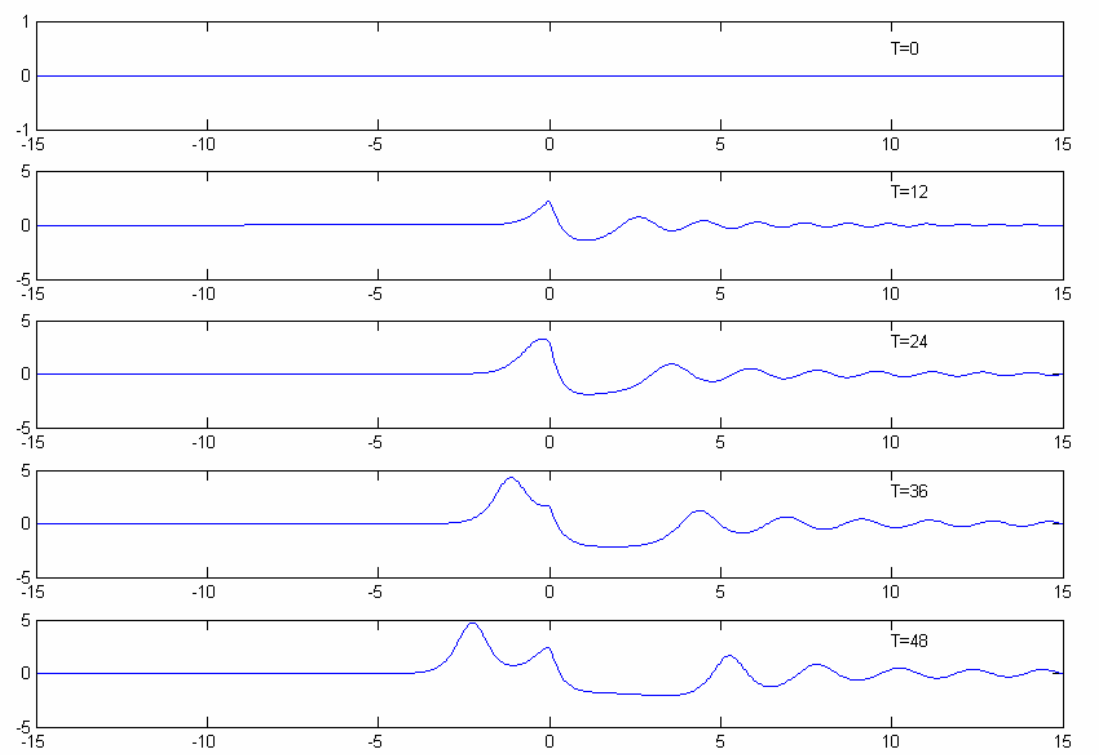

Figure 10 Solution of Eq. (5) with the parameters based on the radiosonde ascent data in Hong Kong at 8 a.m., 22 September 2005.